Design of Transverse Flux Linear Synchronous Generator for Wave Energy Conversion

Ryuji Watanabe[1], Jung-Seob Shin[1], Takafumi Koseki[1], and Houng-Joong Kim[2]
[1] The University of Tokyo, Engineering Building #2 12F 7-3-1 Hongo, Bunkyo-ku, Tokyo 113-8656, Japan
[2] KOVERY Co. Ltd, 19, Jangan-ro, 359, beon-gil, Jangan-gu, Suwon-si, Gyeonggi-do, 440-301, KOREA
E-mail: ryuji@koseki.t.u-tokyo.ac.jp

Abstract — This paper presents the practical rapid design approach for large power density and low cost of transverse flux type permanent magnet linear synchronous generator for wave energy conversion. The proposed design approach is based on response surface methodology and three-dimensional (3D) static analysis. First, the basic structure and operational principle of the proposed model used for wave energy conversion are described. Second, in order to solve the problem that it takes much time to design transverse flux type topologies due to its complex structure, the simplified design approach for large power density and low cost under the condition where motor's structure and total volume are known is proposed. Finally, the result and effiracy of proposed design approach are evaluated by 3D finite element analysis (FEA).

I. INTRODUCTION

Recently, ocean energy conversion has been of great interest in the industrial field. Especially, compared with other renewable energy sources, generation using wave power has been attractive and many researchers have been tried to bring wave power generator into commercial use [1].

Generally, large power density, low cost, and easy maintenance are important technical requirements in order to wave power generation. Considered easy maintenance, wave power generation using linear type generator has a great advantage because the use of gearboxes and rotation-linear conversion are not needed in linear motion [2]. Several types of linear generators are available. In particular, because of the advent of rare-earth permanent magnets [3], a permanent-magnet linear synchronous generator (PMLSG) has been attractive. However, one of the drawbacks of the PMLSG is that the thrust density is comparatively lower than that of rotary generators equipped with rotary-to-linear converters.

Hence, increasing the power density is one of the most important research topics with regard to the PMLSG today. A transverse-flux-type topology is an ideal alternative in which the flux is carried in the iron-back in a plane transverse (perpendicular) to the direction of motion and current flow. Therefore, the magnetic and electric loads in the machine are along different planes. This allows for an inverse relationship to exist between the capability of the machine to produce power and the pole pitch, which results in a higher power density [4]

However, due to the presence of a 3D magnetic circuit, the process for manufacturing conventional transverse-flux-type topologies is generally difficult and it takes much time to design, which limits its application in wave power generation.

In earlier works, the authors have proposed a transverse-flux-type topology using generic armature cores for rotary machinery has been proposed to address the problem of complex structures in conventional transverse-flux-type topologies [5]. Unlike the configuration in conventional transverse-flux-type topologies, the proposed model has a 2-D magnetic circuit in which the main flux flows transversely from the north pole to the south pole along the armature core. In this magnetic circuit, the iron cores in the armature and field units can be easily fabricated using laminated steel plates that are arranged along the moving direction [5].

This paper mainly focuses on three things. First, the basic structure and operational principle of the proposed model which is used for wave power generator are introduced. Second, the practical rapid design approach for the maximum power density in which three-dimensional (3D) static analysis and response surface methodology (RSM) are used and the proposed model is designed by applying the practical rapid design approach. Third, the design results and efficacy of the simplified design approach are analyzed and evaluated.

II. BASIC STRUCTURE

Fig. 1 shows the configuration of the three-phase unit of the proposed model [5]. In the overall configuration, the armature side is the stator, and the field side is the mover, as shown in Fig. 1(a). The armature side consists of armature units in a non-magnetic material box connected to the base stage. The field side consists of field units inside of a stainless steel pipe connected to buoy.

A basic armature unit consists of an even number of salient poles and a concentrated winding structure along with a four-salient-poles configuration, as shown in Fig. 1(b). Every armature coil is wound in series with a phase difference of 180°. By applying a current to these coils, each of them is excited with a phase difference of 180°. In Fig. 1(b), -U denotes the current component shifted by 180° from U. A field unit consists of an even number of field magnets (equal to the number of salient poles in the armature unit) and an iron core, as shown in Fig. 1(b). The field magnets are magnetized along the radial direction, similar to that in a conventional cylindrical structure. In this configuration, not only the

armature core of three-phase machines but also the armature core of the stepping motor can be used as the armature core. Further, the field side is designed according to the shape of the armature core.

When a field unit is accurately located in the center of the armature unit, a magnetic circuit is formed, as shown in Fig. 1(c). The main flux flows transversely from the north pole to the south pole along the armature core. In this manner, the cross-sectional symmetrical magnetic form of the balanced magnetic circuits that have the same number of salient poles in armature unit emerges.

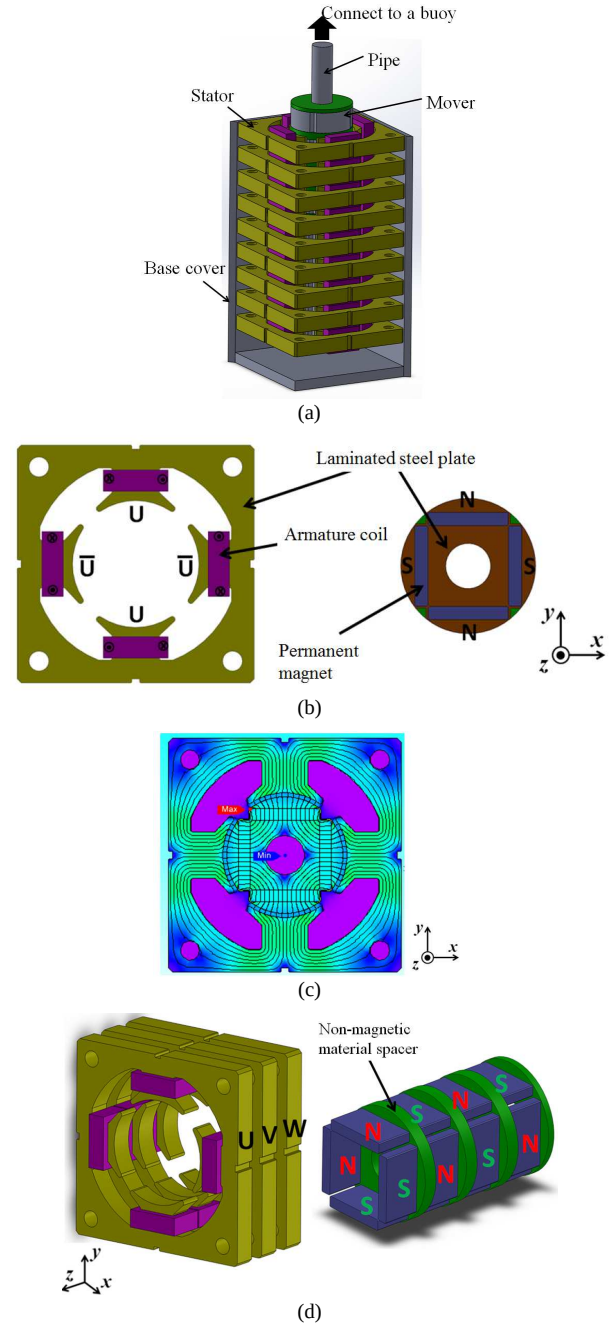

Fig. 1. Fundamental configuration of the three-phase unit. (a) The entire configuration. (b) The armature and field unit. (c) Magnetic circuits. (d) Configuration along moving direction. (In (d), iron cores in the field side have been removed for better understanding and clarity.)

The armature cores are arranged along the direction of movement (i.e., the z-direction), as shown in Fig. 1(d). Each core is spatially separated by a difference of 120°. The field magnets are arranged along the z-direction, and each magnet is electrically separated by 180°. The non-magnetic material spacer isolates the magnetic paths between the iron cores. In this structure, each unit in the armature and field sides is magnetically separated. The flux flow is transverse to the direction of movement and the longitudinal flux flow (similar to that in a conventional cylindrical structure) back to the common core is absent. Therefore, any core-pole combination, including not only the fundamental three core-two pole combination but also the three core-four pole combination, can be easily achieved by arranging each unit in the armature and field sides along the direction of movement.

III. Practical Rapid Design Optimization Using 3D Static Analysis and Response Surface Methodology

In this section, the proposed simplified method using 3D static analysis and response surface methodology is described.

A. Main Parameters in the design approach

Basic specification of proposed model is shown in Table.1. External radius of armature, air gap and diameter of armature conductor is constant values in any cases. The ratio of field core and non-magnet spacer is also the constant value, three to one.

Since 50JN230 (JFE-steel) is used in armature and field core, 1.5T denotes the maximum flux density in the non-saturation region [6]. Material of permanent magnet is N50M, one of the Neodymium magnet that residual magnetic flux density is 1.32T [7].

Fig.5 is design variables of the proposed model. There are three design variables in this model, armature iron core width w, slot pitch τ_s defined as thickness of armature and coil along moving direction, and field radius r. These three design variables are the factors of response surface methodology. All of three factors are the parameter involving electric loading and magnetic loading, therefore, they have direct affect on the output power. The qualitative meaning of the factors is explained as follows:

1). Armature iron core width w: Factor w is related to the magnetic saturation, and one magnetic circuit always has the same width, $w/2$. By this constraint condition, armature iron core width and coil width have relationship of trade-off, that is, electric loading and magnetic loading have relationship of trade-off with changing w.

2). Slot pitch τ_s: From factor w, the coil width is determined. Therefore, according to the increase of τ_s, the thickness of armature increases and magnetic loading increases. By slot combination, pole pitch defined as length field core and spacer along moving direction is determined. With the increase of τ_s, the pole pitch also increases, and drive frequency decreases. As the result, output power has one maximum point with changing τ_s.

3). Field radius *r*: If the field radius increases, the magnet volume increases proportionately, however the iron teeth length winded coil decreases. Therefore, electric loading and magnetic loading have relationship of trade-off with changing *r*.

Table.1 Basic specification of proposal model.

Symbol	Quantity
External radius of armature	275[mm]×275[mm]
Air gap	1[mm]
Diameter of armature conductor	1[mm]
Material	
Armature core	50JN230
Field core	50JN230
Permanent magnet	N50M
Non-magnet spacer	Aluminum
Coil	Copper
Slot combination	3slot-4pole
velocity	0.8m/s

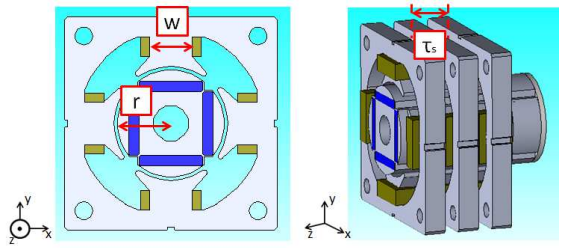

(a) (b)

Fig.5. Design variables of the proposed model. (a) x-y plain. (b) y-z plain.

B. *Estimation Output power using 3D Static analysis*

The flux in field magnet, d-axis and q-axis are obtained by the 3D static analysis and each symbol is ϕ_f, ϕ_d and ϕ_q. This model is a salient pole machine and d-axis armature inductance differs from q-axis armature inductance. The d-axis and q-axis armature inductance, L_d and L_q, are expressed as (1) and (2).

$$L_d = N\frac{\phi_d - \phi_f}{I} \tag{1}$$

$$L_q = N\frac{\phi_q}{I} \tag{2}$$

where *N* and *I* are the armature turns and the armature current. Considering moving direction, when the angular frequency is presented $\omega = 2\pi f$, the air gap flux distribution is expressed as (3).

$$\phi(t) = \phi_f \cos \omega t \tag{3}$$

By differentiating the air gap flux distribution, the no-load induced voltage is expressed as (4) and effective value of (4) is expressed as (5).

$$e(t) = N\omega\phi_f \sin \omega t \tag{4}$$

$$E_f = \frac{\omega N \phi_f}{\sqrt{2}} \tag{5}$$

Fig.2 is phasor diagrams for salient pole type generator operation. In Fig.2, I_d and I_q are the d-axis and q-axis current, and X_d and X_q are reactance expressed as $X_d = \omega L_d$ and $X_q = \omega L_q$. *R* is load resistance and V_{out} is load voltage. Fig.3 shows an equivalent circuit for generator operation. Load is only resistance load as Fig.3, and power factor is considered as 1. The armature winding resistance is expressed as r_a in Fig.3. From Fig.2 and Fig.3, the d-axis and q-axis current obtained are expressed as (6) and (7). Under these condition, output power *P* is calculated as (8).

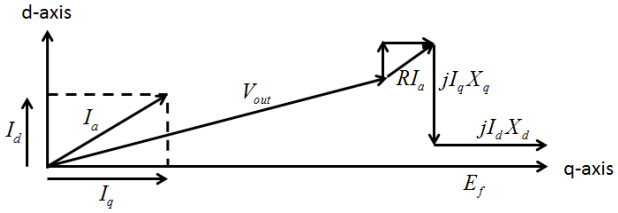

Fig. 2. Phasor diagrams for generator operation.

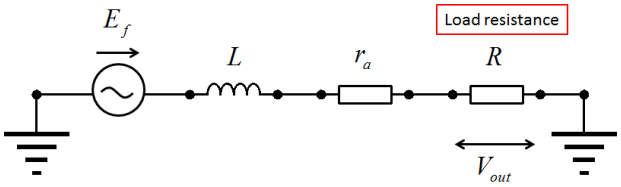

Fig. 3. Equivalent circuit for generator operation.

$$I_d = \frac{(R+r_a)E_f}{(R+r_a)^2 + (X_q - X_d)(R+r_a) - X_q^2} \tag{6}$$

$$I_q = \frac{X_q E_f}{(R+r_a)^2 + (X_q - X_d)(R+r_a) - X_q^2} \tag{7}$$

$$P = E_f I_q - I_d I_q (X_d - X_q) - r_a I_a^2 \tag{8}$$

C. *Response Surface Methodology*

RSM has increasingly been used for optimization problem, because of its efficiency and a small amount of required data [8]. The response is generally obtained from real experiments or computer simulations. Therefore, in this paper, FEA is used as numerical experiments to provide the response. Power density defined as the power per total volume and power per magnet volume are the responses. In order to check magnetic saturation, flux density is also response. They are changed by the design variables variation. The relationship between the response of interest (*y*) and the *k* predictor variables (x_1, x_2, …, x_k) may be known exactly allowing a description of the system of the form [9].

$$y = f(x_1, x_2, \cdots, x_k) + \varepsilon \tag{9}$$

where ε is the random error observed in the response. The form of true response function *f* is unknown and very complicated, so it is approximated. Usually, a low-order polynomial of the independent variables is employed. Therefore, the first or second-order model is used. In this paper, in order to consider two-factor interaction, a second-order model defined as (10) is used.

$$y = \beta_0 + \sum_{i=1}^{k} \beta_i x_i + \sum_{i=1}^{k} \beta_{ii} x_i^2 + \sum_{i<j} \beta_{ij} x_i x_j + \varepsilon \qquad (10)$$

where β is regression coefficient. The observation response vector y at n data point of function y may be written in matrix notation as follows:

$$y = X\beta + \varepsilon \qquad (11)$$

Where X is a matrix of the levels of the independent variables, β is a vector of regression coefficients, and ε is a vector of random error. The least-squares method, which is to minimize the sum of squares of the random errors, is used to estimate unknown vector β. The least-square function L is as follows:

$$L = \sum_{i=1}^{n} \varepsilon_i^2 = \varepsilon^T \varepsilon = \left(y - X\beta\right)^T \left(y - X\beta\right) \qquad (12)$$

where ε^T is the transpose of the matrix ε. known exactly allowing a description of the system of the form.

The estimated vector β' of unknown vector β must satisfy the following equation.

$$\left.\frac{\partial L}{\partial \beta}\right|_{\beta'} = -2X^T y + 2X^T X\beta' = 0 \qquad (13)$$

Therefore, the estimated vector β' can be written as (14) vand the fitted response vector y' is given by (15).

$$\beta' = \left(X^T X\right)^{-1} X^T y \qquad (14)$$

$$y' = X\beta' \qquad (15)$$

where X^T is the transpose of the matrix X.

There are many experimental designs for creation of response surface like D-optimal designs and 3-level full factorial designs [10], [11]. In this paper, in order to estimate interactions of design variables and curvature properties of response surface in a few times of experiments, the central composite design (CCD) is chosen. It is one of the most important and commonly used classes of experimental designs for a second-order response surface [12].

The CCD is composed of the 2^n factorial or fraction of 2^n factorial design with $2n$ axial and n_c central points. The choice of parameter α, the distance of the axial design points from the central design points is also important for adequate performance of CCD. The value of α specifies the location of the axial, which can be chosen by the experimenter to satisfy various conditions. In this paper, α = 2 is chosen, because of obtaining integer parameters in any levels.

It is always necessary to examine the fitted model to ensure that it provides an adequate approximation for response. The total variation is a set of data called the total sum of squares (SST) of deviations of observed Y_u about their average Y.

$$SST = \sum_{u=1}^{N} \left(Y_u - \bar{Y}\right)^2 \qquad (16)$$

where N is the total number of experiments.

The SST can be partitioned into two parts, the sum of squares due to regression (SSR) (or sum of squares explaned by the fitted model) and the sum of squares unaccounted for by the fitted (or sum squares of error (SSE)). The formula for calculate the SSR is as follows:

$$SSR = \sum_{u=1}^{N} \left(Y_u' - \bar{Y}\right)^2 \qquad (17)$$

The deviation is the difference between the predicted value Y_u' by the fitted model in the uth observation and the overall average of the Y_u.

The SSE by the fitted model is as follows:

$$SSE = \sum_{u=1}^{N} \left(Y_u - Y_u'\right)^2 \qquad (18)$$

The coefficient of multiple determination R^2 expressed by SST and SSR is as follows:

$$R^2 = \frac{SSR}{SST} \qquad (19)$$

It is a measure of the proportion of total variation of the values of Y_u about the mean -Y explained by the fitted model. A related statistic, called the adjust coefficients of multiple determination R_A^2 is as follows:

$$R_A^2 = 1 - \frac{SSE/(N-k)}{SST/(N-1)} \qquad (20)$$

where k is the number of parameters in the fitted model. Accordingly, R^2 and R_A^2 are applied to evaluate accuracy of the fitted model in this paper.

D. The process of the proposed method

Fig. 4 shows the flowchart of a design process using response surface methodology.

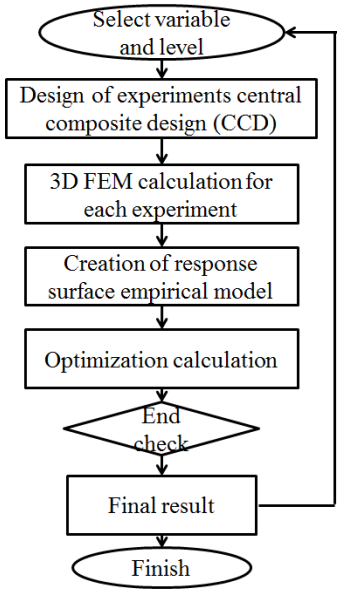

Fig. 4. Flowchart of a design process using response surface methodology.

In Fig. 4, the first step is to decide variables and variable levels. Therefore, the other parameters are constants. When selecting variable, we should care that objective functions with changing the variables have monophasic. In the second step, the values of parameter needed to make response surface are

determined by using CCD. Then, in order to output the objective functions, experiment is done by using 3D static analysis. The next step is creation of response surface and finding the optimum point. Then, whether the optimum point is real point is confirmed by the value of R^2 and R_A^2. In this paper, $0.95 \leq R^2$, $R_A^2 \leq 1.0$ is good value. If optimum point is right, the design flow is finished. If not, from the first step, the flowchart is repeated.

IV. Analysis of the Result

A. *Design of proposed model by using response surface methodology*

Table.2 shows the data table and experimental results using CCD. Experiments from 1 to 15 are selected by CCD, and others are performed in order to improve the value of R^2 and R_A^2. As the objective function, power density and power per magnet volume are shown in the Table.2. The two objective functions are very important to design wave generators, because power density is present total output power in limited space and power per magnet volume is present cost since permanent magnet is expensive. Flux density is also objective function in order not to saturate magnetically.

Response surfaces of these three objective functions and convolved function *D* are shown in Fig. 7 – Fig. 9. Function *D* is made by convolving power density and power per magnet volume in the ratio of one to two in non-saturation region.

From Fig.6 (d), the optimal value for function *D* is 46.5mm. Due to the minimal accuracy of 1mm in the hardware design, *w* is chosen to be 47mm (i.e. round off to 46.5mm). In the same way, from Fig.7 (d) and Fig. 8 (d), τ_s is chosen to be 83mm and *r* is chosen to be 54mm.

Table.2 Data table and experimental results using CCD

Exp	*w* [mm]	τ_s [mm]	*r* [mm]	Power density [W/m^3]	Power per magnet volume [W/m^3]
1	50	80	55	4.43×10^4	1.48×10^6
2	60	80	55	2.67×10^4	8.92×10^5
3	50	90	55	4.05×10^4	1.36×10^6
4	60	90	55	2.52×10^4	8.44×10^5
5	50	80	65	4.83×10^4	1.11×10^6
6	60	80	65	3.73×10^4	8.58×10^5
7	50	90	65	4.75×10^4	1.09×10^6
8	60	90	65	3.65×10^4	8.40×10^5
9	45	85	60	4.96×10^4	1.36×10^6
10	65	85	60	2.48×10^4	6.83×10^5
11	55	75	60	3.87×10^4	1.07×10^6
12	55	95	60	3.49×10^4	9.59×10^5
13	55	85	50	2.85×10^4	1.19×10^6
14	55	85	70	4.78×10^4	9.33×10^5
15	55	85	60	3.65×10^4	1.09×10^6
16	45	65	65	3.40×10^4	7.15×10^5
17	45	65	70	3.07×10^4	4.59×10^5
18	50	80	60	4.65×10^4	1.28×10^6
19	40	85	60	5.46×10^4	1.63×10^6

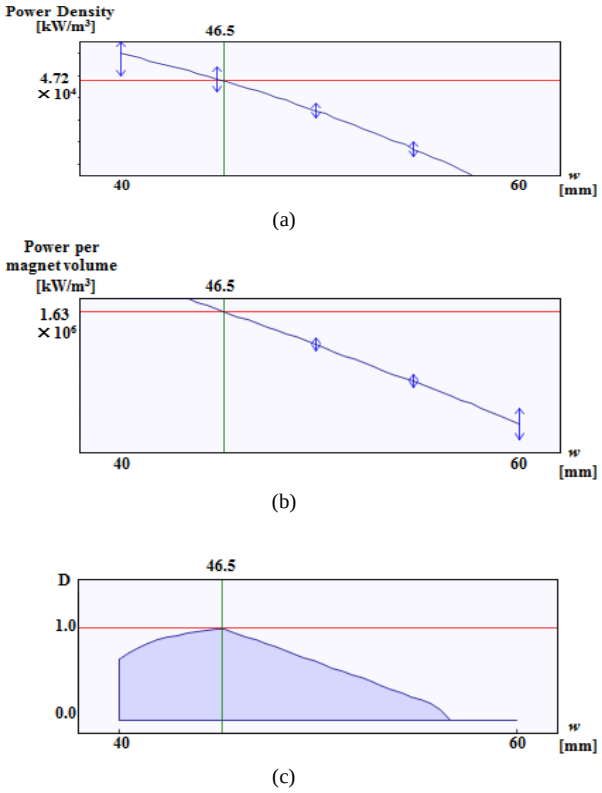

Fig.6. Response surface by *w* factor. (a) power density. (b) power per magnet volume. (c) convolved function *D*.

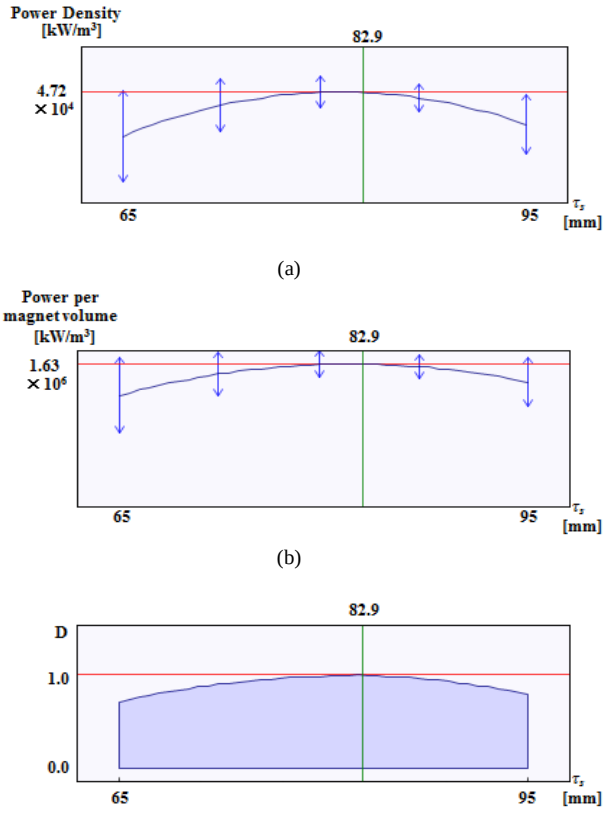

Fig.7. Response surface by τ_s factor. (a) power density. (b) power per magnet volume. (c) convolved function *D*.

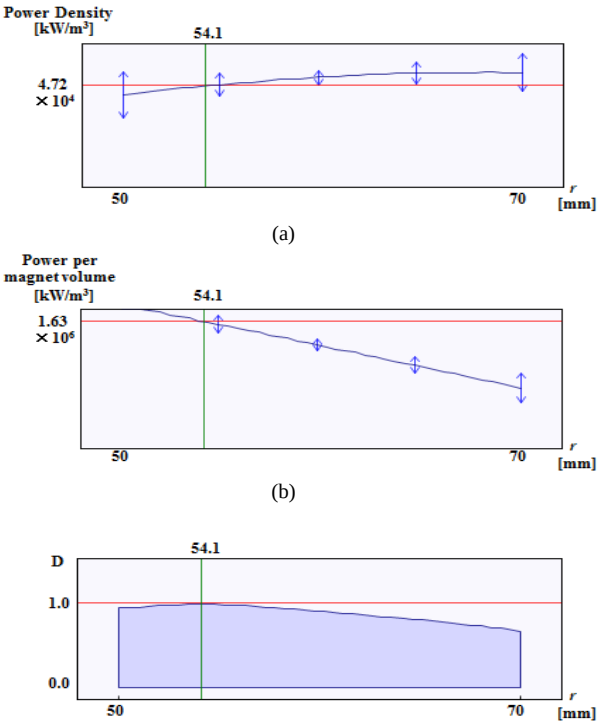

Fig.8. Response surface by *r* factor. (a) power density. (b) power per magnet volume. (c) convolved function *D*.

B. Results and discussion

In the Table.3, the results of design by using response surface methodology are shown. The performance prediction for optimal design has to be checked by carrying out an FEM computations, 3D static analysis and 3D transient response analysis.

Table.3 Comparison of analysis in optimal proposed model.

	Power density [W/m^3]	Power per magnet volume [W/m^3]
Response surface methodology	4.72×10^4	1.63×10^6
3D static analysis	4.70×10^4	1.64×10^6
3D transient response analysis	4.53×10^4	1.54×10^6

The error by response surface methodology is confirmed to be small from the values of power density and power per magnet volume by 3D static analysis. The error by calculation output power using 3D static analysis is also small from the values of power density and power per magnet volume by 3D transient response analysis.

The authors guess that some errors caused by assumption that the air gap flux distribution is sinusoidal wave. However, the optimal criteria are very close to response surface methodology and rapid design and an accurate performance prediction is achieved.

In addition to these results, the analysis time by 3D static analysis is only 10 minutes, on the other hand, the analysis time by 3D transient response analysis is 2 days. Then, the number of experience, 19 times, is drastically decreased by using response surface methodology with CCD compared the case that the searching method have been taken in each 1mm different value of w, τ_s, and r for finding optimal point.

V. CONCLUSION

In this paper, an optimal design process using response surface methodology and 3D static analysis has been introduced to design a TF type linear generator. By using response surface methodology with CCD, the number of numerical experiments is reduced, and by using 3D static analysis, the analysis time is reduced. Then, a large power and low cost model is designed by introducing power density and power per magnet volume as objective function. The validity of the optimal design process is confirmed by FEM analysis. As the result, TF type generator is easily designed by proposed design method considering power density and power per magnet volume.

This optimal model is low space availability, 55% therefore, the power is not enough to bring wave power generator into commercial use. More large power models should be discussed by using proposed method in the future.

REFERENCES

[1] M. Leijon, et al, "Catch the wave to electricity," *IEEE Power Energy Mag*., vol. 7, no. 1, pp. 50–54, Jan./Feb. 2009.

[2] N. Hodgins, O. keysan, A. Mcdonald and M. Mueller, "Linear Generator for Direct Drive Wave Energy Applications," *International Conference on Electrical Machines* (ICEM), 2010.

[3] R. Vartanian, Y. Deshpande and H. A. Toliyat, "Performance analysis of a rare earth magnet based NEMA frame Permanent Magnet assisted Synchronous Reluctance Machine with different magnet type and quantity," *International Electrical Machines and Drives Conference* (IEMDC), 2013.

[4] Y. Ueda, H. Takahashi, T. Akiba and M. Yoshida, "Fundamental Design of a Consequent-Pole Transverse-Flux Motor for Direct-Drive Systems," *IEEE Transactions on Magnetics*, vol. 49, no. 7, pp. 4096-4099, July. 2013.

[5] J. S. Shin, T. Koseki, and H. J. Kim, "Transverse flux type cylindrical linear synchronous motor for large thrust using generic armature cores for rotary machinery," *Proceedings of The 20th International Conference on Electrical Machines* (ICEM), pp.795–800, Sept. 2012.

[6] JFE Steel Corp.
Available: http://www.jfe-steel.co.jp/.

[7] Shin-Etsu Chemical Co., Ltd.
Available: http://www.shinetsu.co.jp/j/index.shtml.

[8] T. Ishikawa, M. Yamada and N. Kurita, "Design of Magnet Arrangement in Interior Permanent Magnet Synchronous Motor by Response Surface Methodology in Consideration of Torque and Vibration," *IEEE Transactions on Magnetics*, vol. 47, no. 5, pp. 1290-1293, May. 2011.

[9] H. M. Hasanien, A. S. Abd-Rabou and S. M. Sakr, "Design Optimization of Transverse Flux Linear Motor for Weight Reduction and Performance Improvement Using Response Surface Methodology and Genetic Algorithms," *IEEE Transactions on Energy Conversion*, vol. 25, no. 3, pp. 598-605, Sept. 2010.

[10] H. Shim, S. Wang and K. Lee, "3-D Optimal Design of Induction Motor Used in High-Pressure Scroll Compressor," *IEEE Transactions on Magnetics*, vol. 45, no. 5, pp. 2076-2084, May. 2009.

[11] J. Chen, D. X. Sun and C. F. J. Wu, "A Catalogue of Two-Level and Three-Level Fractional Factorial Designs with Small Runs," *International Statistical Review*, vol. 61, no. 1, pp. 131-145, Apr. 1993.

[12] J. M. Park, S. I. Kim, J. P. Hong, and J. H. Lee, "Rotor design on Torque Ripple Reduction for a synchronous reluctance motor with concentrated winding using response surface methodology," *IEEE Transactions on Magnetics*, vol. 42, no. 10, pp. 3479–3481, Oct. 2006.